

Pion-nucleon scattering in a Bethe-Salpeter approach

A.D. Lahiff^a, I.R. Afnan^b

^a*TRIUMF, 4004 Wesbrook Mall, Vancouver, B.C., Canada V6T 2A3*

^b*School of Chemistry, Physics and Earth Sciences, The Flinders University of South Australia, GPO Box 2100, Adelaide 5001, Australia*

(Received: November 19, 2018)

A covariant model of elastic pion-nucleon scattering based on the Bethe-Salpeter equation is presented. We obtain a good description of the S - and P -wave phase shifts up to 360 MeV laboratory energy. We also compare results from the K -matrix approach and several 3-dimensional quasipotential equations to the Bethe-Salpeter equation.

1 Introduction

Over the past decade many dynamical models of pion-nucleon (πN) scattering based on meson-exchange have been developed. These models invariably begin with an effective hadronic Lagrangian describing the couplings between the various mesons and baryons. The tree-level diagrams obtained from this Lagrangian are then unitarized using an approximation to the Bethe-Salpeter equation (BSE) [1], such as the K -matrix approach or a 3-dimensional (3-D) quasipotential equation. The 3-D reduction procedure is ambiguous because there are an infinite number of different quasipotential equations [2, 3], each having different off-shell behaviour [4]. There is no overwhelming reason to choose one quasipotential equation over another. Sometimes quasipotential equations have been devised so as to have the correct one-body limit, however this argument has been shown to be not applicable to πN scattering [5]. Furthermore, many of the commonly used quasipotential equations violate charge-conjugation symmetry [6]. Here we avoid these problems by constructing a covariant model of elastic πN scattering [7] based on the BSE, which we solve without making any approximations to the relative-energy dependence of the kernel.

2 The model

The BSE for the $\pi N \rightarrow \pi N$ amplitude T is

$$T(q', q; P) = V(q', q; P) - \frac{i}{(2\pi)^4} \int d^4 q'' V(q', q''; P) G_{\pi N}(q''; P) T(q'', q; P), \quad (1)$$

where $G_{\pi N}$ is the 2-body πN propagator. In principle, both the π and N propagators should be fully dressed, but for only 2-body unitarity to be maintained, $G_{\pi N}$ has the simple form

$$G_{\pi N}(q; P) = \frac{1}{(\mu_\pi P - q)^2 - m_\pi^2 + i\epsilon} \frac{\mu_N \not{P} + \not{q} + m_N}{(\mu_N P + q)^2 - m_N^2 + i\epsilon}, \quad (2)$$

where μ_N and μ_π are functions of $s = P^2$ such that $\mu_N + \mu_\pi = 1$. The solution of the BSE does not depend on the choice of $\mu_N(s)$ and $\mu_\pi(s)$, so we use the simplest possibility: $\mu_N = \mu_\pi = 1/2$. The interaction kernel V is truncated to include only the 2nd order $\pi N \rightarrow \pi N$ diagrams obtained from the following interaction Lagrangian:

$$\begin{aligned} \mathcal{L}_{\text{int}} = & \frac{f_{\pi NN}}{m_\pi} \bar{N} \gamma_5 \gamma^\mu \boldsymbol{\tau} N \cdot \partial_\mu \boldsymbol{\pi} + \mathcal{L}_{\pi N \Delta} + g_{\sigma NN} \bar{N} N \sigma + \frac{g_{\sigma \pi \pi}}{2m_\pi} \sigma \partial_\mu \boldsymbol{\pi} \cdot \partial^\mu \boldsymbol{\pi} \\ & + g_{\rho NN} \bar{N} \frac{1}{2} \boldsymbol{\tau} \cdot \left(\gamma_\mu \boldsymbol{\rho}^\mu + \frac{\kappa_\rho}{2m_N} \sigma_{\mu\nu} \partial^\mu \boldsymbol{\rho}^\nu \right) N + g_{\rho \pi \pi} \boldsymbol{\rho}^\mu \cdot (\boldsymbol{\pi} \times \partial_\mu \boldsymbol{\pi}). \end{aligned} \quad (3)$$

Due to the ambiguity in the description of spin-3/2 particles, we consider two different possibilities for the $\pi N\Delta$ vertex:

$$\mathcal{L}_{\pi N\Delta}^{\text{conv}} = \frac{f_{\pi N\Delta}}{m_\pi} \bar{\Delta}^\mu (g_{\mu\nu} + x_\Delta \gamma_\mu \gamma_\nu) \mathbf{T}N \cdot \partial^\nu \boldsymbol{\pi} + \text{h.c.}, \quad (4)$$

$$\mathcal{L}_{\pi N\Delta}^{\text{Pas}} = \frac{f_{\pi N\Delta}}{m_\pi m_\Delta} \epsilon^{\mu\nu\alpha\beta} (\partial_\mu \bar{\Delta}_\nu) \gamma_5 \gamma_\alpha \mathbf{T}N \cdot \partial_\beta \boldsymbol{\pi} + \text{h.c.} \quad (5)$$

Here $\mathcal{L}_{\pi N\Delta}^{\text{conv}}$ is the conventional $\pi N\Delta$ vertex which contains the so-called off-mass-shell parameter x_Δ , while $\mathcal{L}_{\pi N\Delta}^{\text{Pas}}$ is the Pascalutsa vertex [8]. For the Δ propagator we use the standard Rarita-Schwinger (RS) form [9]. It is well known that the RS spin-3/2 propagator contains off-mass-shell spin-1/2 components. The use of the Pascalutsa $\pi N\Delta$ vertex, together with the RS Δ propagator, ensures that the s - and u -channel Δ poles present in V are free of any contributions from the spin-1/2 components of the RS Δ propagator.

	conventional		Pascalutsa	
	model I	model II	model I	model II
$g_{\pi NN}^2/4\pi$	13.5	13.5	13.5	13.5
$g_{\pi NN}^{(0)2}/4\pi$	1.80	4.68	12.1	6.64
$f_{\pi N\Delta}^2/4\pi$	0.365	0.365	0.741	0.63
$f_{\pi N\Delta}^{(0)2}/4\pi$	0.37	0.20	0.193	0.1
x_Δ	-0.11	-0.24	—	—
$g_{\rho\pi\pi}g_{\rho NN}/4\pi$	2.88	2.63	2.73	2.25
κ_ρ	2.66	2.03	4.11	4.97
$g_{\sigma\pi\pi}g_{\sigma NN}/4\pi$	-0.41	0.39	-3.80	-4.65
$m_N^{(0)}$	1.34	1.14	1.72	1.18
$m_\Delta^{(0)}$	2.305	1.492	2.60	1.498
m_σ	0.65	0.62	0.69	1.12
Λ_N	3.17	—	4.90	—
Λ_Δ	4.56	—	3.20	—
Λ_π	1.77	1.85	1.76	2.08
Λ_ρ	3.67	—	3.06	—
Λ_σ	1.30	—	4.26	—

Table 1: The coupling constants and particle masses resulting from fits to the πN data using the two different form factor parameterizations (denoted as model I and model II), and the two different $\pi N\Delta$ vertices. The quantities in boldface were varied in the fits. All masses are in GeV.

Regularization is achieved by the introduction of form factors. We consider two different parameterizations: in model I we associate a cutoff function with each vertex, where this cutoff function is taken as the product of form factors that depend on the 4-momentum squared of each particle present at the vertex. In model II, we associate a form factor only with the pion propagator. In both models, each form factor is chosen to have the form:

$$f(q_a^2) = \left(\frac{\Lambda_a^2 - m_a^2}{\Lambda_a^2 - q_a^2} \right)^{n_a}. \quad (6)$$

This form factor fulfils the requirement of only having poles along the real axis. In this work we use $n_{\text{all}} = 1$ for model I, and $n_\pi = 8$ for model II.

We solve the BSE by first expanding the nucleon propagator in the πN intermediate states into positive and negative energy components, and then sandwiching the resulting equation between Dirac spinors. This gives two coupled 4-D integral equations which are reduced to 2-D integral equations after partial wave decomposition. A Wick rotation [10] is performed in order to obtain equations suitable for numerical solution. This means that all amplitudes are analytically continued in the relative-energy variables from the real axis to the imaginary axis, thereby avoiding the singularities of the kernel. Form factors with poles only along the real axis do not interfere with the Wick rotation provided the cutoff masses are large enough [7].

3 Numerical results

The free parameters are determined in χ^2 fits to the S - and P -wave phase shifts up to 360 MeV pion laboratory energy from the SM95 partial wave analysis [11]. The parameters obtained are shown in Table 1. Note that $g_{\pi NN}$ was fixed at $g_{\pi NN}^2/4\pi = 13.5$, while $g_{\pi NN}^{(0)}$ and $m_N^{(0)}$ were determined by the nucleon renormalization procedure [7]. This ensures that in the P_{11} partial wave the dressed s -channel nucleon pole diagram has a pole at the physical nucleon mass with a residue related to the physical πNN coupling constant.

The resulting phase shifts are shown in Figure 1. When the conventional $\pi N\Delta$ vertex is used, we obtain very good agreement with the partial wave analysis. There is some disagreement in the P_{11} partial wave when the the Pascalutsa $\pi N\Delta$ vertex is used, which suggests that the spin-1/2 components of the RS Δ propagator are necessary in order to obtain a good fit to the πN data. Note that the model II results are very close to the model I results, even though model II has four less free parameters. Therefore in our framework the use of a different cutoff mass for each particle results in unnecessary free parameters. The scattering lengths and volumes are shown in Table 2, where it is seen that we obtain reasonable agreement with the partial wave analyses.

Our coupling constants are consistent with the commonly accepted values in the literature, with the exception of $f_{\pi N\Delta}$ when the Pascalutsa $\pi N\Delta$ vertex is used. In this case, the $\pi N\Delta$ coupling constant is around twice as large as the so-called ‘‘empirical’’ value obtained from the decay $\Delta \rightarrow \pi + N$, i.e., $f_{\pi N\Delta}^2/4\pi = 0.36$. Notice in Table 1 that the choice of form factor parameterization does not have a significant effect on the values of the ρ and σ coupling constants. However, the choice of the $\pi N\Delta$ vertex does make a difference to κ_ρ and $g_{\sigma\pi\pi}g_{\sigma NN}$. It has been shown that Δ pole diagrams constructed using the conventional and Pascalutsa $\pi N\Delta$ vertices differ by a contact term [13]; in our models it appears that this contact term is partially being mimicked by the ρ and σ exchange diagrams.

ℓ_{2I2j}	BSE (conv)	BSE (Pas)	SM95	KH80
S_{11}	0.177	0.172	0.175	0.173
S_{31}	-0.101	-0.105	-0.087	-0.101
P_{11}	-0.083	-0.058	-0.068	-0.081
P_{13}	-0.032	-0.031	-0.022	-0.030
P_{31}	-0.041	-0.041	-0.039	-0.045
P_{33}	0.178	0.187	0.209	0.214

Table 2: Scattering lengths and volumes obtained from the BSE in units of $m_\pi^{-(2\ell+1)}$, compared to results from the SM95 [11] and KH80 [12] πN partial wave analyses. The model I form factor parameterization was used.

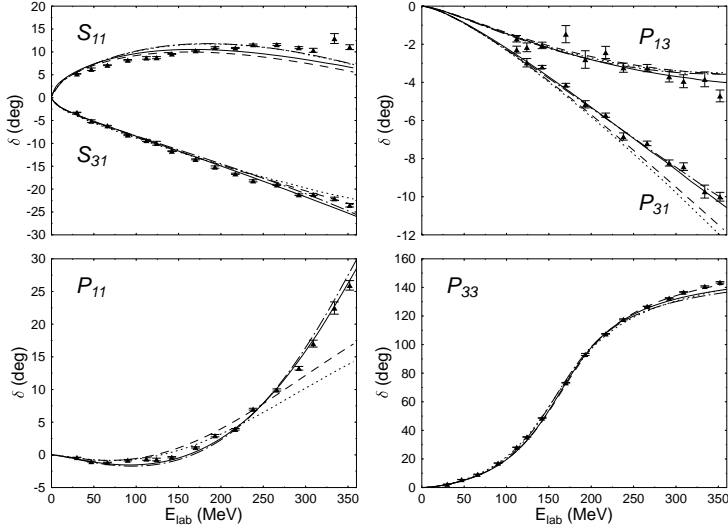


Figure 1: Phase shifts obtained from the BSE using the conventional $\pi N\Delta$ vertex [model I (solid line), model II (dot-dashed line)], and the Pascalutsa $\pi N\Delta$ vertex [model I (dashed line), model II (dotted line)]. The data points are from the SM95 partial wave analysis [11].

4 Approximations to the Bethe-Salpeter equation

The BSE has not often been used in meson-exchange models to describe meson-baryon or baryon-baryon scattering processes. Due to the relative-energy integration, the BSE is usually regarded as being too hard to solve, so it has been much more common to use various approximations to the BSE. The K -matrix approach is the simplest method, where a unitary T matrix is found directly from the on-shell potential via

$$T = V - i \text{Im}[G_{\pi N}] V. \quad (7)$$

This is obtained from the BSE when the principle-value parts of all loop diagrams are neglected. In Figure 2 we compare the K -matrix approach to the BSE, with the parameters obtained from the BSE fits used in the K -matrix approach calculations. For P_{13} and P_{31} the K -matrix results agree fairly well with the BSE. The results for the remaining partial waves illustrate the importance of dressing and multiple scattering: the K -matrix results deviate significantly from the BSE results. Note that for the model II form factors the K -matrix approach does slightly better than for model I, i.e., dressing and multiple scattering are more important in model I than in model II. This is due to the large size of the cutoff masses in the model I fit as compared to the cutoff mass in the model II fit (see Table 1).

Another approach is to approximate the relative-energy integration in the BSE in some way, resulting in a 3-D quasipotential equation. Note that many quasipotential equations depend on the choice of μ_N and μ_π [as defined in Eq. (2)] due to the violation of Lorentz-invariance. Here we consider the usual choice

$$\mu_N(s) = \frac{s + m_N^2 - m_\pi^2}{2s}, \quad \mu_\pi(s) = \frac{s + m_\pi^2 - m_N^2}{2s}. \quad (8)$$

In the Cohen equation [14] it is assumed that the T matrix is independent of the relative-energy, and so the relative-energy integration can be performed explicitly over V and $G_{\pi N}$, resulting in a 3-D equation. In Salpeter's instantaneous equation [15], it is assumed that the interaction kernel is independent of the relative-energy, hence allowing the relative-energy integration to be performed explicitly over just $G_{\pi N}$. There are an infinite number of possible 3-D equations which are obtained from the BSE by replacing $G_{\pi N}$ by an approximate 2-body propagator which generates the πN unitarity cut, but contains a δ -function on the relative-energy. The Blankenbecler-Sugar (BbS)

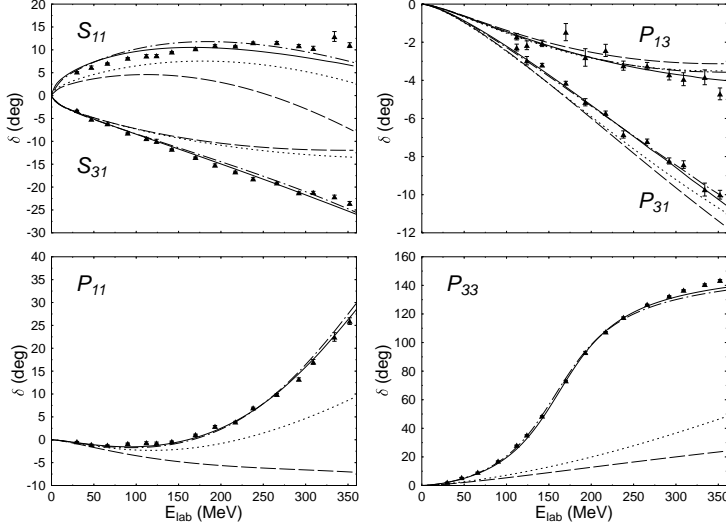


Figure 2: Comparison between the BSE [model I (solid line), model II (dot-dashed line)], and the K -matrix approximation [model I (dashed line), model II (dotted line)]. The conventional $\pi N \Delta$ vertex was used.

equation [16] uses the following propagator:

$$G_{\pi N}^{\text{BbS}}(q; P) = 2\pi i \int_{s_{th}}^{\infty} \frac{ds' f(s', s)}{s' - s - i\epsilon} [\mu_N \not{P}' + \not{q} + m_N] \delta^{(+)}[(\mu_N P' + q)^2 - m_N^2] \delta^{(+)}[(\mu_\pi P' - q)^2 - m_\pi^2], \quad (9)$$

where $s_{th} = (m_N + m_\pi)^2$, and the function $f(s', s)$ is taken as unity. We note that the choice of f is in fact arbitrary, provided $f(s, s) = 1$, hence allowing for the possibility of an infinity of different equations. Different choices for μ_N and μ_π also result in different equations. The Cooper-Jennings (CJ) equation [17] makes use of the propagator

$$G_{\pi N}^{\text{CJ}}(q; P) = 2\pi i [\mu_N \not{P}' + \not{q} + m_N] \int_{s_{th}}^{\infty} \frac{ds' f(s', s)}{s' - s - i\epsilon} \delta^{(+)}[(\mu_N P' + q)^2 - m_N^2] \delta^{(+)}[(\mu_\pi P' - q)^2 - m_\pi^2], \quad (10)$$

where f is chosen such that $G_{\pi N}^{\text{CJ}}$ can be rewritten as

$$G_{\pi N}^{\text{CJ}}(q; P) = 2\pi i \frac{\delta(2P \cdot q)}{q^2 - k^2} [\mu_N \not{P}' + \not{q} + m_N], \quad (11)$$

with $k^2 = m_N^2 - s\mu_N^2(s)$.

Using the parameters obtained in the BSE fits to the πN partial wave analysis, we calculate phase shifts using the four different quasipotential equations and compare the results to the BSE. In Figure 3 we see that all four of the considered 3-D equations agree reasonably well with the BSE in the S_{31} , P_{13} and P_{31} partial waves. In the P_{11} partial wave, the Cohen and instantaneous equations agree well with the BSE results, but the Blankenbecler-Sugar and Cooper-Jennings equations generate far too much attraction. For P_{33} only the Cohen equation gives phase shifts with the same shape as the BSE results. The other three equations produce so much attraction that the $\Delta(1232)$ resonance has become a bound state, therefore causing the phase shifts at the πN threshold to be 180° , rather than 0° .

The agreement between the Cohen equation and the BSE is not surprising, and has been found before in $\phi\phi$ scattering [18]. The relative-energy integration over $V G_{\pi N}$ produces 4-body as well as 2-body thresholds. Consequently, the T matrix obtained from the Cohen equation contains more of the analytic structure generated by the BSE as compared to the other quasipotential equations considered here, which only contain the 2-body threshold.

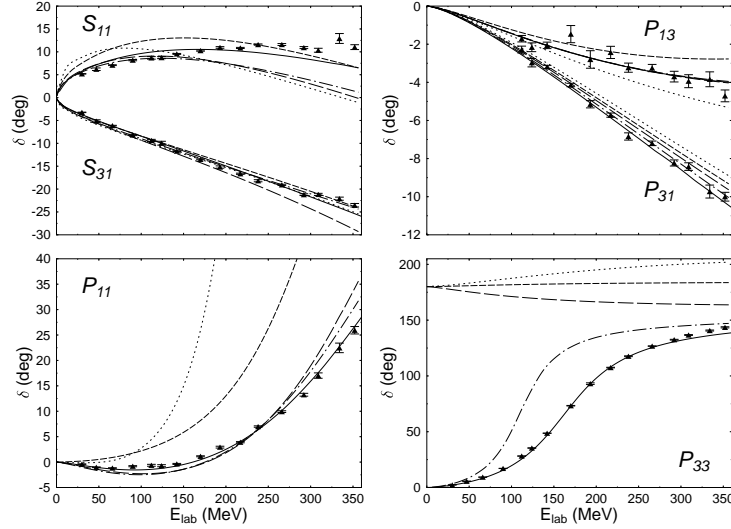


Figure 3: Comparison between the Bethe-Salpeter (solid line), Cohen (dot-dashed line), Salpeter (long-dashed line), Blankenbecler-Sugar (short-dashed line), and Cooper-Jennings (dotted line) equations. The conventional $\pi N \Delta$ vertex was used, with the model I form factor parameterization.

5 Concluding remarks

In summary, we have presented a relativistic description of πN scattering based on the Bethe-Salpeter equation, which we have compared to some approximations schemes, including the K -matrix approach and four different 3-D quasipotential equations. In some partial waves large differences were found between the BSE and the other approaches.

The present model could be extended to higher energies by including resonances into the interaction kernel and couplings to inelastic channels, or extended to include the photon so as to give a covariant model of pion photoproduction including final-state interactions. Work in both these directions is in progress.

Acknowledgments: This work was supported by the Australian Research Council. We also acknowledge the South Australian Centre for Parallel Computing for access to their computing facilities.

References

- [1] E. E. Salpeter and H. A. Bethe, Phys. Rev. **84**, 1232 (1951).
- [2] R. J. Yaes, Phys. Rev. D **3**, 3086 (1971).
- [3] A. Klein and T. -S. H. Lee, Phys. Rev. D **10**, 4308 (1974).
- [4] C. Hung, S. N. Yang and T. -S. H. Lee, Phys. Rev. C **64**, 034309 (2001).
- [5] V. Pascalutsa and J. A. Tjon, Phys. Rev. C **60**, 034005 (1999).
- [6] V. Pascalutsa and J. A. Tjon, Phys. Lett. B **435**, 245 (1998).
- [7] A. D. Lahiff and I. R. Afnan, Phys. Rev. C **60**, 024608 (1999).
- [8] V. Pascalutsa, Phys. Rev. D **58**, 096002 (1998).
- [9] W. Rarita and J. Schwinger, Phys. Rev. **60**, 61 (1941).
- [10] G. C. Wick, Phys. Rev. **96**, 1124 (1954).
- [11] R. A. Arndt, I. I. Strakovsky, R. L. Workman and M. M. Pavan, Phys. Rev. C **52**, 2120 (1995).
- [12] R. Koch and E. Pietarinen, Nucl. Phys. A **336**, 331 (1980).
- [13] V. Pascalutsa, Phys. Lett. B **503**, 85 (2001).
- [14] H. Cohen, Phys. Rev. D **2**, 1738 (1970).
- [15] E. E. Salpeter, Phys. Rev. **87**, 328 (1952).
- [16] R. Blankenbecler and R. Sugar, Phys. Rev. **142**, 1051 (1966).
- [17] E. D. Cooper and B. K. Jennings, Nucl. Phys. A **500**, 553 (1989).
- [18] R. M. Woloshyn and A. D. Jackson, Nucl. Phys. B **64**, 269 (1973).